Article

SOURCE DATA TRANSPARENT PROCESS OPEN ACCESS

EMBO Molecular Medicine

Attenuation of clinical and immunological outcomes during SARS-CoV-2 infection by ivermectin

Guilherme Dias de Melo[1], Françoise Lazarini[2], Florence Larrous[1], Lena Feige[1], E
Sylvain Levallois[5], Agnès Marchio[6], Lauriane Kergoat[1], David Hardy[7], Thomas C
Pascal Pineau[6], Marc Lecuit[5,8], Pierre-Marie Lledo[2], Jean-Pierre Changeux[9] & Her

Abstract

The devastating pandemic due to SARS-CoV-2 and the emergence of antigenic variants that jeopardize the efficacy of current vaccines create an urgent need for a comprehensive understanding of the pathophysiology of COVID-19, including the contribution of inflammation to disease. It also warrants for the search of immunomodulatory drugs that could improve disease outcome. Here, we show that standard doses of ivermectin (IVM), an anti-parasitic drug with potential immunomodulatory activities through the cholinergic anti-inflammatory pathway, prevent clinical deterioration, reduce olfactory deficit, and limit the inflammation of the upper and lower respiratory tracts in SARS-CoV-2-infected hamsters. Whereas it has no effect on viral load in the airways of infected animals, transcriptomic analyses of infected lungs reveal that IVM dampens type I interferon responses and modulates several other inflammatory pathways. In particular, IVM dramatically reduces the *Il-6/Il-10* ratio in lung tissue and promotes macrophage M2 polarization, which might account for the more favorable clinical presentation of IVM-treated animals. Altogether, this study supports the use of immunomodulatory drugs such as IVM, to improve the clinical condition of SARS-CoV-2-infected patients.

Keywords coronavirus; inflammation; ivermectin; SARS-CoV-2; viral infections
Subject Categories Immunology; Microbiology, Virology & Host Pathogen Interaction
DOI 10.15252/emmm.202114122 | Received 11 February 2021 | Revised 22 June

Introduction

Coronaviruses cause respiratory disease i
During the ongoing pandemic of SARS-C
disease 19 (COVID-19), clinical signs oth
toms have been linked to infection, fr
neurological symptoms such as anosmia a
have been related to an over-responsive
system to SARS-CoV-2 (Bhaskar *et al*, 20
et al, 2020). Consequently, there is an u
the hallmarks of this over-responsiveness
peutics or repurpose drugs to improve
COVID-19 patients (Batalha *et al*, 2021).

Ivermectin (IVM), a macrocyclic lacton
able anti-parasitic drug which prevents in
endo- and ectoparasites (Sajid *et al*, 200
2020). IVM is an efficient positive allost
nicotinic acetylcholine receptor (nAChR) (
several ligand-gated ion channels, includi
glutamate (GluCl) in worms (Hibbs & Gou
IVM has been shown to exert an imm
humans and animals (Sajid *et al*, 2006; Hei
under conditions that are known to involve
Tracey, 2012), even though its underlying
established (Laing *et al*, 2017). A direct
SARS-CoV-2 with nAChR has also been h
because of sequence homologies between S
and nAChR ligands such as snake venom

reported to reduce viral load and improve the clinical status of mice infected by an animal coronavirus, the mouse hepatitis virus (MHV) (Arévalo *et al*, 2021). *In vitro* inhibition of SARS-CoV-2 replication by IVM in Vero/hSLAM cells has also been reported (Caly *et al*, 2020), albeit at much higher concentrations (50- to 100-fold) than those clinically attainable in humans (150–400 µg/kg) (Guzzo *et al*, 2002; Bray *et al*, 2020; Chaccour *et al*, 2020).

The aim of this study is to investigate pathogenesis of COVID-19, in a SARS-Cc golden Syrian hamster. This species is na virus and the most reliable and affordable 19 (Chan *et al*, 2020; Muñoz-Fontela *et al* recently used to demonstrate the impc inflammation with intranasal administratic

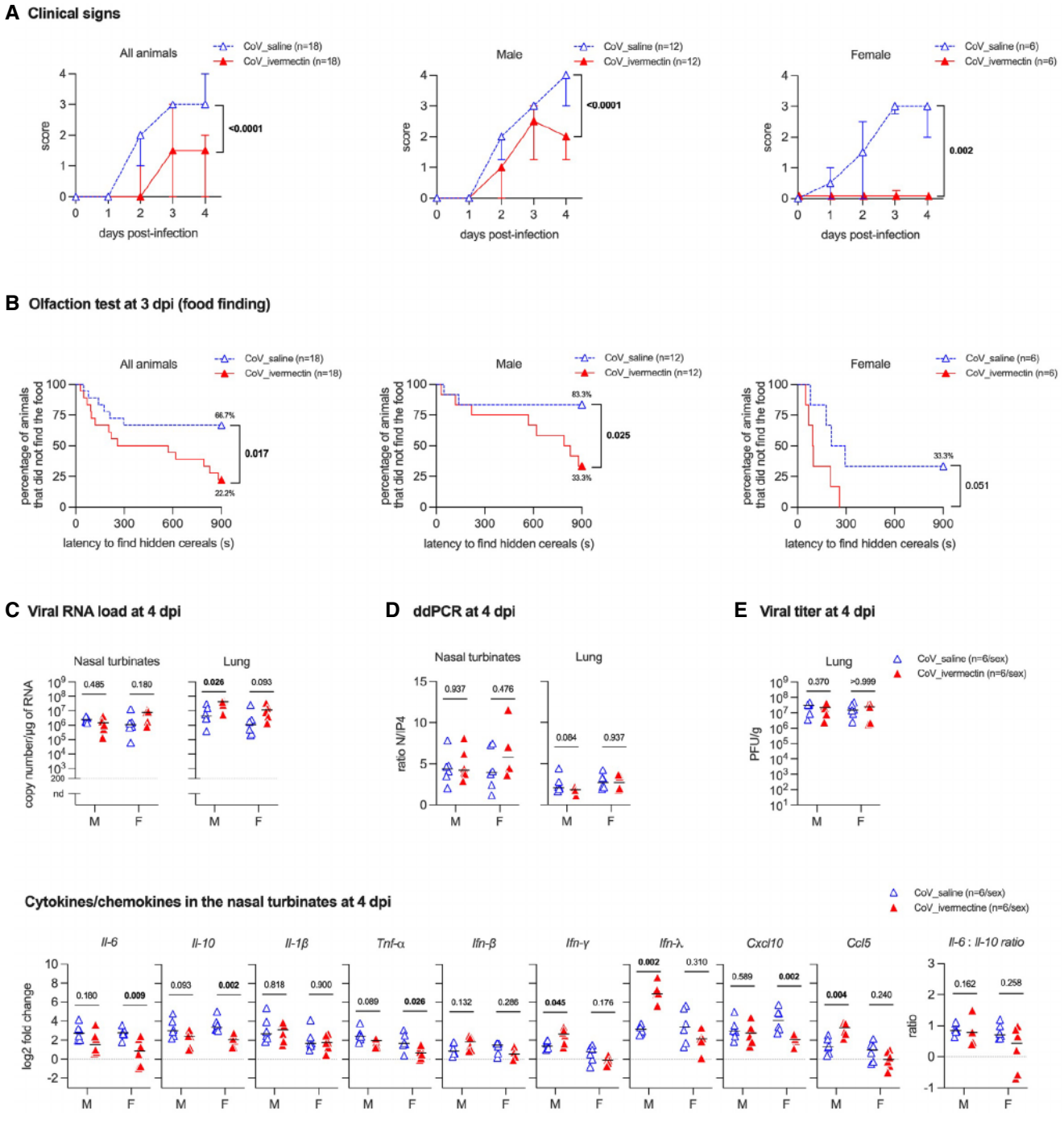

Guilherme Dias de Melo et al E

Figure 1. Clinical presentation, olfaction test, viral load and immune profile in the nasal turbinates of SARS-CoV-2-infected ham ivermectin treatment.

A Clinical signs in infected hamsters. The clinical score is based on a cumulative 0–4 scale: ruffled fur; slow movements; apathy; and absen Symbols indicate the median ± interquartile range.

B Olfactory performance in infected hamsters. The olfaction test is based on the hidden (buried) food finding test. Curves represent the per not find the buried food. Food finding assays were performed at 3 days post-infection (dpi). Data were obtained from three independent two independent experiments for females.

C Viral load in the nasal turbinates and in the lungs at 4 dpi.

D Ratio between the CPD (copy per droplets, normalized to *γ-actin* and *Hprt* reference gene relative expression) of structural [N, nucleocaps RdRp, RNA-dependent RNA polymerase] viral gene expression determined by digital droplet PCR (ddPCR) in the nasal turbinates and in t

E Infectious viral titer in the lung at 4 dpi expressed as plaque-forming units (PFU)/g of tissue.

F Cytokine and chemokine transcripts in the nasal turbinates at 4 dpi in male and female SARS-CoV-2-infected hamsters, treated with sali ivermectin.

Data information: Horizontal lines indicate medians. The *P* value is indicated in bold when significant at a 0.05 threshold. Mann–Whitney te (Mantel–Cox) test (B). M: male hamsters and F: female hamsters. Data were obtained from two independent experiments for each sex. See F Appendix Fig S1.
Source data are available online for this figure.

disease progression (Hoagland *et al*, 2020). Male and female adult golden Syrian hamsters were intranasally inoculated with 6×10^4 PFU of SARS-CoV-2 [BetaCoV/France/IDF00372/2020]. This inoculum size was selected as it invariably causes symptomatic infection in golden Syrian hamster, with a high incidence of anosmia and high viral loads in the upper and lower respiratory tracts within 4 days post-inoculation (dpi) (de Melo *et al*, 2021). At the time of infection, animals received a single subcutaneous injection of IVM at the anti-parasitic dose of 400 μg/kg, commonly used in human clinical setting, and were monitored over 4 days.

Here, we show that the modulation of the host's inflammatory response using IVM as a repurposed drug strongly diminished the clinical score and severity of the disease (including anosmia) observed in these animals, although it has no impact on viral load. IVM-treated animals presented a strong modulation in several signaling pathways, including a significant reduction of the type I and III interferon response and of the *Il-6/Il-10* ratio, along with the presence of M2 macrophages in the lung. These effects were mostly compartmentalized and sex-dependent, and treated infected females exhibited better clinical outcomes.

Results and Discussion

COVID-19 clinical outcome is attenuated by ivermectin

In order to study the effects of IVM chemical therapy on clinical outcome, we assessed body weight, clinical score, and olfactory

significantly reduced clinical score, and it in infected females (Fig 1A). Remarkably the olfactory deficit in infected animals 66.7% (12/18) of the saline-treated infe with hyposmia/anosmia, whereas only 22. infected hamsters presented with signs (Figs 1B and EV1B–D). The olfactory per enced by sex: 83.3% (10/12) of the sali presented with hyposmia/anosmia, agair IVM-treated infected males (Figs 1B and E 33.3% (2/6) of saline-treated infected hyposmia/anosmia, no olfactory deficit treated infected females (0/6; Figs 1B and I

Since males presented a higher incider we subsequently performed a dose-respor of IVM on the clinical presentation an infected males: Lower doses of IVM (100 c lar clinical outcomes as the anti-parasiti EV2). As expected, no signs of olfactory mock-infected hamsters (Fig EV1B–D).

Ivermectin treatment does not influence respiratory tract of infected hamsters

To evaluate the effect of IVM treatment respiratory tract, we tested the nasal turbir hamsters using both classical RT–qPCR sensitive technique of digital droplet PCR

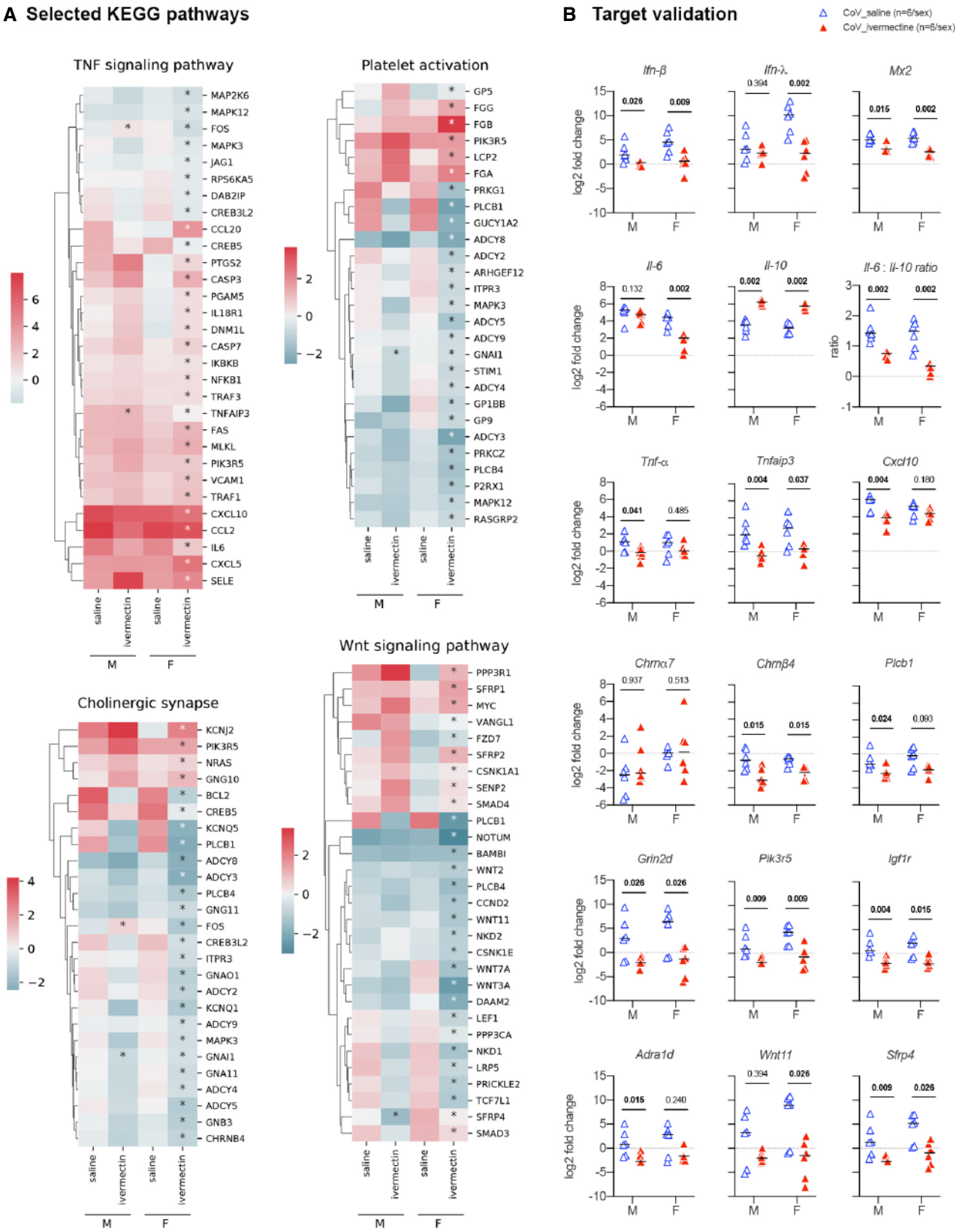
A Selected KEGG pathways
TNF signaling pathway
MAP2K6
MAPK12
FOS
MAPK3
JAG1
RPS6KA5
DAB2IP
CREB3L2
CCL20
CREB5
PTGS2
CASP3
PGAM5
IL18R1
DNM1L
CASP7
IKBKB
NFKB1
TRAF3
TNFAIP3
FAS
MLKL
PIK3R5
VCAM1
TRAF1
CXCL10
CCL2
IL6
CXCL5
SELE
saline
ivermectin
saline
ivermectin
M
F
Platelet activation
GP5
FGG
FGB
PIK3R5
LCP2
FGA
PRKG1
PLCB1
GUCY1A2
ADCY8
ADCY2
ARHGEF12
ITPR3
MAPK3
ADCY5
ADCY9
GNAI1
STIM1
ADCY4
GP1BB
GP9
ADCY3
PRKCZ
PLCB4
P2RX1
MAPK12
RASGRP2
Cholinergic synapse
KCNJ2
PIK3R5
NRAS
GNG10
BCL2
CREB5
KCNQ5
PLCB1
ADCY8
ADCY3
PLCB4
GNG11
FOS
CREB3L2
ITPR3
GNAO1
ADCY2
KCNQ1
ADCY9
MAPK3
GNAI1
GNA11
ADCY4
ADCY5
GNB3
CHRNB4
Wnt signaling pathway
PPP3R1
SFRP1
MYC
VANGL1
FZD7
SFRP2
CSNK1A1
SENP2
SMAD4
PLCB1
NOTUM
BAMBI
WNT2
PLCB4
CCND2
WNT11
NKD2
CSNK1E
WNT7A
WNT3A
DAAM2
LEF1
PPP3CA
NKD1
LRP5
PRICKLE2
TCF7L1
SFRP4
SMAD3
B Target validation
CoV_saline (n=6/sex)
CoV_ivermectine (n=6/sex)
Ifn-β
Ifn-λ
Mx2
Il-6
Il-10
Il-6 : Il-10 ratio
Tnf-α
Tnfaip3
Cxcl10
Chrnα7
Chrnβ4
Plcb1
Grin2d
Pik3r5
Igf1r
Adra1d
Wnt11
Sfrp4
log2 fold change
ratio
M
F

Figure 2. Transcriptomic profile in the lung of SARS-CoV-2-infected hamsters with and without ivermectin treatment at 4 days

A Heatmaps showing the differentially expressed genes according to the selected KEGG pathways calculated in comparison with mock-infe Benjamini–Hochberg-adjusted *P*-value < 0.05 in the comparison between saline and ivermectin within the same sex. Color gradient repre fold change comparing infected and mock-infected. Complete analyses are listed in Dataset EV1.

B Validation targets in the lung at 4 dpi. Horizontal lines indicate medians. The *P* value is indicated in bold when significant at a 0.05 thres

Data information: M: male hamsters and F: female hamsters. Data were obtained from two independent experiments for each sex. See Figs E Source data are available online for this figure.

Ivermectin therapy modulates local immune responses in infected hamsters' nasal turbinates

Anosmia is a typical symptom of COVID-19 in humans, with some sex-dependent differences (Han *et al*, 2020; Qiu *et al*, 2020; Xydakis *et al*, 2020). Inflammation in the nasal cavity, following olfactory sensory neurons infection and deciliation, has been shown to be an underlying factor for smell loss during SARS-CoV-2 infection (de Melo *et al*, 2021), and the chemokine *Cxcl10* could be directly implicated due to its neurotoxic potential (Oliviero *et al*, 2020). We therefore tested a possible modulation by IVM of the local inflammatory response in hamsters and in particularly in the nasal turbinates, the primary target tissue of SARS-CoV-2 infection (de Melo *et al*, 2021), that could correlate its effect on the olfactory score. To this aim, a panel of cytokines (*Il-6, Il-10, Il-1β, Tnf-α, Ifn-β, Ifn-γ,* and *Ifn-λ*) and chemokines (*Cxcl10* and *Ccl5*) were used to assess the impact of IVM treatment on immune responses in the nasal turbinates of SARS-CoV-2-infected hamsters at 4 dpi. Upon treatment with IVM, females presented a significant downregulation of *Il-6, Il-10, and Tnf-α*, which are key inflammatory mediators of prognostic value in COVID-19 patients (McElvaney *et al*, 2020a), and of *Cxcl10* (Fig 1F), in line with their better olfactory performance observed in the food finding tests (Fig 1B). The differences between sex groups are illustrated by the increase in three pro-inflammatory mediators (*Ifn-γ*, *Ifn-λ*, and *Ccl5*) only in males (Fig 1F). No difference for the *Il-6/Il-10* ratio was observed in the nasal turbinates.

Lung immunometabolism is affected by SARS-CoV-2 infection and modulated by ivermectin

IVM attenuates lung pathology and inflammation pathways, including cholinergic synapse-related genes

In order to further study the mode of action of IVM on clinical signs, we performed at 4 dpi a comparative agnostic transcriptomic approach using RNA-seq in the lower respiratory tract in hamsters

only 36 downregulated and 51 upregulate
the lungs of IVM-treated males. This sex di
by KEGG and GO enrichments representati

Several KEGG pathways were signifi
treated females: "TNF signaling path
synapse", in line with the activation of vag
inflammatory pathway (CAP) (Pavlov & T
Di Giovanni, 2020), and "platelet activati
of thrombosis (Zhang *et al*, 2020b; Chen &
EV4A). We also observed a modulation of
way" KEGG pathway in the IVM treatme
shown to correlate with lung homeostasis
& Yoon, 2020), obesity, type-2 diabetes,
2014; Aamir *et al*, 2020) (Figs 2A and E
pathways in IVM-treated female hamster
"vascular smooth muscle contraction", an
cardiomyocytes" which could be related t
constriction and therefore attenuation of l
(Potus *et al*, 2020; Vaduganathan *et al*, 2
drate metabolism and insulin resistan
observed in RNA-seq analyses of the lung
SARS-CoV-2 infection, linked to hy
syndrome, and impairments in the imm
what is observed in COVID-19 in humans
Gianchandani *et al*, 2020). In IVM-treated
females, the term "insulin resistance" was
KEGG enrichment, and the insulin secretio
ulated. Several other related pathways
inflammation, and lung pathology were
Rap1, AGE-RAGE, and cGMP-PKG signalin
EV5) (Oczypok *et al*, 2017; Pei *et al*, 202
IVM-treated males, significant modulated
KEGG and GO enrichments were related to
and epithelial cells (Fig EV4).

Additionally, the GO enrichment in IVM

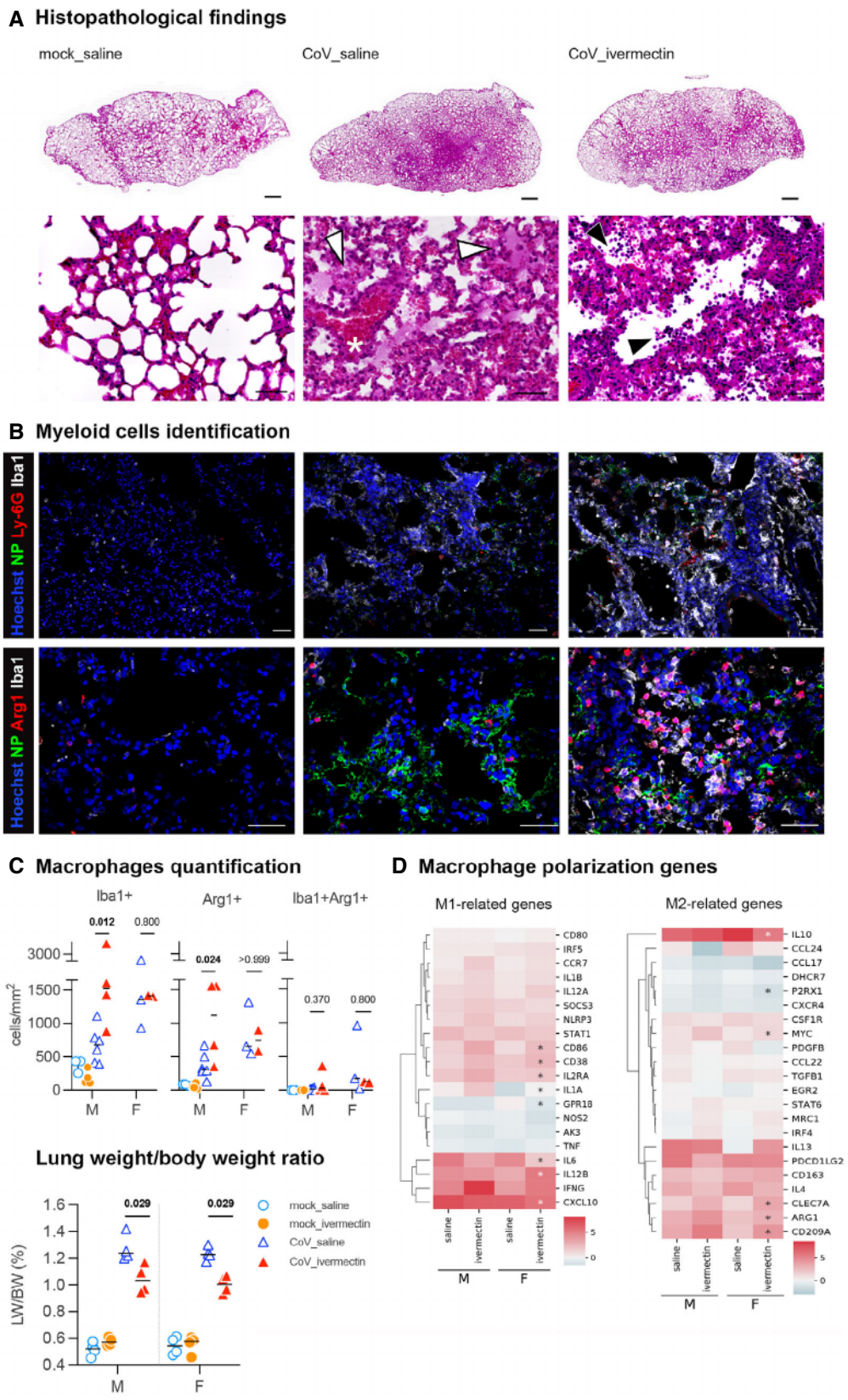
A Histopathological findings
mock_saline
CoV_saline
CoV_ivermectin
B Myeloid cells identification
Hoechst NP Ly-6G Iba1
Hoechst NP Arg1 Iba1
C Macrophages quantification
Iba1+
Arg1+
Iba1+Arg1+
cells/mm²
0.012
0.800
0.024
>0.999
0.370
0.800
M
F
Lung weight/body weight ratio
LW/BW (%)
0.029
0.029
mock_saline
mock_ivermectin
CoV_saline
CoV_ivermectin
D Macrophage polarization genes
M1-related genes
M2-related genes
CD80
IRF5
CCR7
IL1B
IL12A
SOCS3
NLRP3
STAT1
CD86
CD38
IL2RA
IL1A
GPR18
NOS2
AK3
TNF
IL6
IL12B
IFNG
CXCL10
IL10
CCL24
CCL17
DHCR7
P2RX1
CXCR4
CSF1R
MYC
PDGFB
CCL22
TGFB1
EGR2
STAT6
MRC1
IRF4
IL13
PDCD1LG2
CD163
IL4
CLEC7A
ARG1
CD209A
saline
ivermectin

Figure 3. Identification of macrophages in the lung of SARS-CoV-2-infected hamsters with and without ivermectin treatment an transcriptomic profile related to M1/M2 polarization.

A Representative histopathology photomicrographies of lungs according to the different groups: mock_saline, CoV_saline, and CoV_ivermec sections. Bottom panels: high magnification. CoV_saline section exhibits important congestion (*), edema associated with few mononucl Note the thickening of the alveolar walls. CoV_ivermectin section exhibits important amounts of mononuclear cells (black arrowheads) a congestion or edema. Hematoxylin and eosin. Scale bars = 1 mm (top panels) and 20 μm (bottom panels).

B Representative immunofluorescence photomicrographies of neutrophils (Ly-6G), monocytes/macrophages (Iba1), M2 macrophages (Arg1), lung. Scale bars = 50 μm.

C Quantification of Iba1$^+$ cells, Arg1$^+$ cells, and Iba1$^+$Arg1$^+$ cells in the lungs. mock_saline n = 3 (males), mock_ivermectin n = 4 (males), Co females), and CoV_ivermectin n = 6 (4 males and 2 females).

D Heatmaps showing the differentially expressed genes related to the M1/M2 polarization in comparison with mock-infected hamsters. *in Hochberg-adjusted P-value < 0.05 in the comparison between saline and ivermectin within the same sex. Color gradient represents the t comparing infected and mock-infected. Complete analyses are listed in Dataset EV1.

E Lung weight-to-body weight ratio in the different groups (n = 4/sex/group).

Data information: M: male hamsters and F: female hamsters. Horizontal lines indicate medians. The P value is indicated in bold when signifi Mann–Whitney test (C, E).
Source data are available online for this figure.

pathways that were highly regulated in IVM-treated females and we compared by RT–qPCR their respective transcription levels in the lungs of the different groups of animals. Among these genes, several were also significantly modulated between IVM- and saline-treated infected males including *Tnfaip3*, *Sfrp4*, *Epha2*, *Gnai1*, *Hgf*, and *Fos*. Others presented a similar regulation in males compared to females (from KEGG and GO enrichments) although their modulation was not invariably significant: *Casp3, Plcb1, Chrna7, Chrnb4, Adra1d, Grin2d/Nmdar2d, Grid1, Gabrr1, Pik3r5, Igf1r, Wnt11, Wnt3a, Il-2, Il-2ra, Prkg1, Krt4, Creb5, and Ager*. The modulation of these targets, together with other genes from relevant inflammatory mediators taken from the literature (Boudewijns *et al*, 2020; Hoagland *et al*, 2020) (*Il-6, Il-10, Il-1β, Tnf-α, Ifn-β, Ifn-λ, Ifn-γ, Tgf-β, Cxcl10, Ccl5*, and *Mx2)*, was confirmed by RT–qPCR (Figs 2B and EV5).

IVM limited the expression of *Ifn-β* (males and females), *Ifn-λ* (females), and IFN-stimulated gene *Mx2* (males and females) in the lung of infected and IVM-treated hamsters compared to infected and saline-treated hamsters. In contrast, saline-treated hamsters presented an increased expression of *Ifn-β*, *Ifn-λ*, and *Mx2* compared to non-infected hamsters (males and females). This is expected as type I and III IFN signaling pathways have already been shown to correlate with lung pathology severity in SARS-CoV-2-infected hamsters, possibly resulting from a STAT2-dependent response (Boudewijns *et al*, 2020). In contrast, type I and III IFNs are differently expressed in the nasal turbinates, where *Ifn-λ* is upregulated in treated males (Fig 1F). This difference between upper and lower airways may be explained by two factors: (i) the specificity of *Ifn-λ*

effect may be related to a modulation of tl in the lung (downregulation of *Tnf-α* in sexes, and *Il-6* in females) associated wi *Tnf-α* reduction and better clinical pr features caused by the IVM treatment in avirus infection, where mice were infected 2021). Additionally, differently from the n *10* ratio in the lung of IVM-treated hamste than in non-treated animals (Fig 2B), w comparatively better clinical presentation. *Il-6/Il-10* ratios were detected in hospita who did not require intensive care (McEl vaney *et al*, 2020b).

IVM increases the infiltration of monocyt promote M2 polarization in the lung of SA hamsters

To assess directly lung pathology in infect histopathological analyses. The lungs of saline-treated hamsters exhibited substanti of edema, congestion, microhemorrhages, clear cells, hyaline membranes, alveolar in line with previous reports (Chan *et al*, contrast, the lungs of SARS-CoV-2-in hamsters exhibited with reduced degrees yet with greater amounts of mononuclear (Fig 3A). SARS-CoV-2 infection caused

treated animals, along with the reduction of key M1 pro-inflammatory mediators, such as *Il-6, Tnf-α*, and *Cxcl10* (Fig 2B), in similar ways as observed in other viral infections (Sang *et al*, 2015).

Whereas few Iba1$^+$ cells were observed in mock-infected animals, most likely resident interstitial and alveolar macrophages, we observed a large number of Iba1$^+$ myeloid cells in the lungs of IVM-treated animals (Fig 3B). No distinguishable differences were observed in neutrophils population (Ly-6G$^+$) between saline-treated and IVM-treated animals (Fig 3B). Part of these Iba1$^+$ cells were also Arg1$^+$ cells (Fig 3B), a marker of M2-polarized macrophages. IVM treatment was associated with an increase of both Iba1$^+$ and Arg1$^+$ cells in the lungs of SARS-CoV-2-infected male hamsters (Fig 3C). In contrast, in females, while infection promoted an increase of both Iba1$^+$ and Arg1$^+$ cells (Fig 3C), IVM had no impact on the recruitment of these cells. Additionally, RNA-seq analyses in the lung identified the upregulation of key M2-related genes (*Arg1, Cd209a/DC-SIGN, Clec7a/Dectin-1,* and *Myc/c-Myc*) along with classical M1 markers (*Cd86* and *Cd38*; Fig 3D), giving additional support to the M2 polarization tendency caused by the IVM treatment.

Conclusions

Our results demonstrate that IVM improves clinical outcome in SARS-CoV-2-infected animals and is associated with a reduced inflammatory status, but with no impact of SARS-CoV-2 loads in the upper and lower respiratory tracts. Thus, in hamsters, as in humans (preprint: Cereda *et al*, 2020; Hasanoglu *et al*, 2021), symptomatology and therefore the severity of SARS-CoV-2 infection is not strictly correlated with viral load. The main effect of IVM in the lungs is on type I and III IFN responses and other related signaling pathways including phospholipases, kinases, and adenylate cyclases, which are important therapeutic targets (Melotti *et al*, 2014; Raker *et al*, 2016; Hu *et al*, 2020; Li *et al*, 2020; preprint: Masood *et al*, 2020; Isidori *et al*, 2021), and this translates clinically into an improved clinical score.

The results presented herein are consistent with a role of type I and III IFN responses in the pathogenesis of SARS-CoV-2-associated lung disease in hamsters. They show that IVM administration limits IFN response and lung inflammation, even though defects in the type I IFN pathways have been associated with severe COVID-19 (Bastard *et al*, 2020; Zhang *et al*, 2020a). This result may suggest that while IFN signaling is crucial to control viral replication and prevent severe disease, in infected hamsters, which only develop a moderate disease, IFN signaling may actually increase tissue

2021) and to be potentially beneficial o
patients. Along the same line, we noticed
that IVM treatment increased the gene
Nfe2l2) in the lungs of female hamste
(Dataset EV1), which gives additional ev
upstream activity of IVM during SARS-CoV
data show that these effects are compar
upper and lower respiratory tracts of har
to IVM treatment.

Considerable sex differences are obse
presentation, inflammatory profile, and tr
the lungs of hamsters, as seen in COVID-1
men tend to develop more severe diseas
2020; Takahashi *et al*, 2020), possibly i
signaling (vom Steeg & Klein, 2019; Samu
2020). Interestingly, sex steroids, here fem
influence both the course of COVID-19 in
of IVM, possibly due to the potentiation of
females, such as nAChRs (Krause *et al*, 19
GlyRs (Van Den Eynden *et al*, 2009; Cerd
IVM is a positive allosteric modulator.

Moreover, the data presented herein
reported in human clinical trials with IV
humans, IVM is widely used as anti-helm
therapeutic doses (150–400 μg/kg) (Guzz
the range of those used in our hamster exp
clinical trials on COVID-19 using IVM ha
IVM has been associated with reduction
and disease severity (preprint: Hill *et al*,
Interestingly, in a long-term care facil
received IVM to control a scabies outbr
COVID-19 was observed (Bernigaud *et al*
been administered to hospitalized COVID-
ing outcomes: one study related no efficac
tion (8–18 days after symptom onset) in
treated in combination with other dru
azithromycin, tocilizumab, steroids) (
whereas another study reported lower mor
COVID-19 patients treated with IVM in ad
(hydroxychloroquine, azithromycin, or b
Importantly, in a study that administered
symptom onset, the authors noticed an
anosmia/hyposmia in the IVM group wi
positivity between IVM and placebo group

The presently available data support th

(Lifschitz *et al*, 2000), simulations using a minimal physiologically based pharmacokinetic (mPBPK) model revealed that the lungs would be exposed to IVM concentrations 2.7× greater than those found in the plasma (Jermain *et al*, 2020). Yet, this dose did not suffice to achieve the range of antiviral concentrations reported *in vitro* (Caly *et al*, 2020).

Consequently, considering the results observed in the golden hamster model, IVM may be considered as a therapeutic agent against COVID-19, which would not strongly affect SARS-CoV-2 replication but limit the pathophysiological consequences of the infection *in vivo,* potentially mediated by type I and III IFN responses and several other related signaling pathways, and a favorable M1/M2 myleoid cells ratio in the lungs. A characteristic modulation of the immune response in the lower airways was observed in IVM-treated hamsters characterized by a transcriptomic profile similar to that observed in humans exhibiting less severe symptoms and a better prognosis (preprint: Masood *et al*, 2020; McElvaney *et al*, 2020b). Our data are consistent with the hypothesis that this effect is mediated by the cholinergic anti-inflammatory action of IVM on the vagus nerve reflex (Changeux *et al*, 2020; Tizabi *et al*, 2020), that should be addressed experimentally. In particular, the precise contribution of the nAChR in IVM action should be elucidated in comparison with that of other possible IVM targets (Zemkova *et al*, 2014). Altogether, this study brings the proof of concept that an IVM-based immunomodulatory therapy improves the clinical condition of SARS-CoV-2-infected hamsters, and in clinical trials, it alleviates symptoms of COVID-19 in humans and possibly limits post-COVID-19 syndrome (also known as long COVID) via an anti-inflammatory action.

Materials and Methods

Ethics

All animal experiments were performed according to the French legislation and in compliance with the European Communities Council Directives (2010/63/UE, French Law 2013–118, February 6, 2013) and according to the regulations of Pasteur Institute Animal Care Committees. The Animal Experimentation Ethics Committee (CETEA 89) of the Institut Pasteur approved this study (200023; APAFIS#25326-2020050617114340 v2) before experiments were initiated. Hamsters were housed by groups of 4 animals in isolators and manipulated in class III safety cabinets in the Pasteur Institute animal facilities accredited by the French Ministry of Agriculture for

SARS-CoV-2 model and ivermectin treatn

Male and female Syrian hamsters (*Mes*
AURA) of 5–6 weeks of age (average
purchased from Janvier Laboratories an
pathogen-free conditions. The animals w
lated in isolators in a Biosafety level-3
access to water and food. Before manipul
an acclimation period of 1 week.

Animals were anesthetized with an ir
200 mg/kg ketamine (Imalgène 1000, Meri
(Rompun, Bayer) and received one single
200 µl of freshly diluted ivermectin (I88
classical anti-parasitic dose of 400 µg/kg
100–200 µg/kg for the dose–response
animals received one single subcutaneo
physiological solution. 100 µl of physiolo
6×10^4 PFU of SARS-CoV-2 was then ad
each animal (50 µl/nostril). Mock-infect
physiological solution only.

Infected and mock-infected animals
isolators, and all hamsters were followed
which the body weight and the clinical sc
cal score was based on a cumulative 0–
movements, apathy, and absence of explor

At day 3 post-infection (dpi), animals
test to assess olfaction as previously descr
de Melo *et al*, 2021). Briefly, 24 h befor
fasted and then individually placed into
cm) with clean standard bedding for 10 mi
were placed in another similar cage for 2 m
of cereals were hidden in 1.5 cm bedding i
The tested hamsters were then placed in th
latency to find the food (defined as the t
start digging) was recorded using a ch
carried out during a 15-min period. As soo
hamsters were removed from the cage. O
performed the same test but with visibl
tioned upon the bedding. The tests were
Biosafety level-3 facility that were specially

At 4 dpi, animals were euthanized wit
(ketamine and xylazine) and exsanguina
samples of nasal turbinates and lungs we
ately frozen at −80°C. Fragments of lung
fixed in 10% neutral buffered formalin.

(QuantStudio 6 Flex, Applied Biosystems). Briefly, 2.5 µl of cDNA (12.5 ng) was added to 7.5 µl of a master mix containing 5 µl of Power SYBR Green Mix (4367659, Applied Biosystems) and 2.5 µl of nuclease-free water with nCoV_IP2 primers (nCoV_IP2-12669Fw: 5′-ATGAGCTTAGTCCTGTTG-3′; nCoV_IP2-12759Rv: 5′-CTCCCTTTGT TGTGTTGT-3′) at a final concentration of 1 µM (WHO, 2020). The amplification conditions were as follows: 95°C for 10 min, 45 cycles of 95°C for 15 s and 60°C for 1 min; followed by a melt curve, from 60 to 95°C. Viral load quantification of hamster tissues was assessed by linear regression using a standard curve of eight known quantities of plasmids containing the *RdRp* sequence (ranging from 10^7 to 10^0 copies). The threshold of detection was established as 200 viral copies/µg of RNA. The Golden hamster gene targets were selected for quantifying host inflammatory mediator transcripts in the tissues using the *Hprt* (hypoxanthine phosphoribosyltransferase), the *γ-actin,* and/or the actinB genes as reference (Appendix Table S1). Variations in gene expression were calculated as the *n*-fold change in expression in the tissues from the infected hamsters compared with the tissues of the uninfected ones using the $2^{-\Delta\Delta C_t}$ method (Pfaffl, 2001).

Droplet digital PCR (ddPCR)

Reverse transcription

200 ng of RNA was reverse-transcribed using iScript Advanced cDNA Synthesis kit for RT–qPCR (1702537, Bio-Rad) according to the manufacturer's specifications.

*Quantitative PCR for γ-*actin *and Hprt reference genes*

Real-time PCR was performed in a CFX96 qPCR machine (Bio-Rad). All samples were measured in duplicate. The 10 µl PCR included 0.8 ng of cDNA, 1× PowerUp PCR master mix (A25742, Applied Biosystems), and 0.5 µM of each primer (Appendix Table S1). The reactions were incubated in a 96-well optical plate at 95°C for 2 min, followed by 40 cycles of 95°C for 15 s and 60°C for 1 min.

Droplet digital PCR

ddPCRs were performed on the QX200 Droplet Digital PCR system according to the manufacturer's instructions (Bio-Rad). Briefly, reaction mixture consisted in 10 µl ddPCR Supermix for probe no dUTP (1863023, Bio-Rad), 0.25-1 ng of cDNA, primers and probes for E/IP4 and N/nsp13 duplex reactions used at concentration listed in Appendix Table S2 in a final volume of 20 µl. PCR amplification was conducted in a iCycler PCR instrument (Bio-Rad) with the following condition: 95°C for 10 min, 40 cycles of 94°C for 30 s with a ramping

(15140148, Thermo Fisher) in Lysing (116923050-CF, MP Biomedicals) using (MP Biomedicals) and the following schem m/s during 20 s, incubation at 4°C during nization at 4.0 m/s during 20 s. The tu 10,000 *g* during 1 min at 4°C, and the sup Vero-E6 cells by classical plaque assays (Avicel, RC581-NFDR080I, DuPont) (Baer

Transcriptomics analysis in golden hamst

RNA preparation was used to construct cDNA libraries according to the manufactu Stranded mRNA sample prep kit, Illumin sequencer was used to sequence libraries. performed with the Sequana framework (used the RNA-seq pipeline (v0.9.16), w (https://github.com/sequana/sequana_rna Snakemake 5.8.1 (Köster & Rahmann, 20 from adapters using Cutadapt 2.10 (Martin to the golden hamster MesAur1.0 genome using STAR 2.7.3a (Dobin *et al*, 2012). F *et al*, 2014) was used to produce the count features using annotation MesAur1.0.10 information. Quality control statistics MultiQC 1.8 (Ewels *et al*, 2016). Statistic matrix was performed to identify differ comparing infected versus non-infected samples and separating by sex. Clustering was assessed using a principal component tial expression testing was conducted usi (Love *et al*, 2014) scripts based on SARToo indicating the significance (Benjamini–Ho false discovery rate FDR < 0.05) and the e each comparison. Finally, enrichment anal modules from Sequana, first by converting ids to gene names and then using human and KEGG pathways. The GO enrichmen (Mi *et al*, 2019) and QuickGO (Huntley KEGG pathways enrichment uses gseapy ng/GSEApy/), EnrichR (Chen *et al*, 2013), 2000), and BioMart services. All programm web services were performed via BioServic

Histopathology

Guilherme Dias de Melo et al E

incubating sections for 20min in citrate buffer pH 6.0 (C-9999, Sigma-Aldrich) at 96°C for 20 min. Sections were then blocked in PBS supplemented with 10% goat serum, 4% fetal calf serum, and 0.4% Triton X-100 for 2 h at room temperature, followed by overnight incubation at 4°C with primary antibodies: rat anti-Ly6G (1/100, 551459, BD-Biosciences), chicken anti-Iba1 (1/500, 234006, Synaptic Systems), rabbit anti-Arg1 (1/250, PA5-29645, Invitrogen), and rabbit anti-SARS-CoV nucleoprotein (1/500, provided by Dr Nicolas Escriou, Institut Pasteur, Paris). After rinsing, slides were incubated with the appropriate secondary antibodies (1/500: goat anti-rat Alexa Fluor 546, A11081, Invitrogen; goat anti-rabbit Alexa Fluor 488, A11034, Invitrogen; goat anti-chicken Alexa Fluor 647, A32933, Invitrogen) for 2 h at room temperature. All sections were then counterstained with Hoechst (H3570, Invitrogen), rinsed thoroughly in PBS, and mounted in Fluoromount-G (15586276, Invitrogen) before observation with a Zeiss LM 710 inverted confocal microscope through a Plan Apochromat 20x/0.8 Ph2 M27 lens. Cell quantification was performed in an automated manner using ImageJ. Single-channel images were extracted, thresholded, and converted to binary images. Cells were then counted using the *Particles Analyzer* ImageJ plug-in.

Statistics

Statistical analysis was performed using Prism software (GraphPad, version 9.0.0, San Diego, USA), with $P < 0.05$ considered significant. Quantitative data were compared across groups using log-rank test or two-tailed Mann–Whitney test. Randomization and blinding were not possible due to pre-defined housing conditions (separated isolators between infected and non-infected animals). *Ex vivo* analysis was blinded (coded samples). All animals were included, and data were provided from 2 replications, except food finding in males, that were replicated 3 times.

Data availability

The datasets produced in this study are available in the following databases: RNA-seq: ArrayExpress E-MTAB-10128 (https://www.ebi.ac.uk/arrayexpress/experiments/E-MTAB-10128/).

Expanded View for this article is available online.

The paper explained

Problem
The current pandemic of COVID-19 has cau
deaths and more than 150 million laborator
wide since December 2019 (as of May 20
SARS-CoV-2, commonly brings about upper
symptoms and in severe cases can lead to
death. Different therapeutic approaches hav
this disease but comprehensive therapeutic s

Results
We report that ivermectin, used at the stanc
400 μg/kg, protects infected hamsters from
and from losing the sense of smell during
treated animals exhibited a specific inflamm
a reduced type I/III interferon stimulation an
intracellular signaling pathways, with an in
Il-6/Il-10 ratio and promoting M2 polari
recruited to the lung. These effects are st
with treated females exhibiting the best ou
mectin treatment did not limit viral replica
treated animals presented similar amounts o
cavity and in the lungs.

Impact
The results of this study establish that irre
symptoms and severity of COVID-19 highlig
by host inflammatory response in COVID-
that reduced type I/III interferon and *Il-6/Il-1*
macrophages might account for a more fa
tion, contributing to a better understanding
ology. Ivermectin might then be considered
agent against COVID-19 with no impact o
but alleviating inflammation and ensuing sy

Acknowledgements
The SARS-CoV-2 strain was supplied by the National Reference Centre for

Escriou Innovation laboratory: Vaccines, Institut F
the anti-SARS-CoV-2 nucleoprotein antibody. We
Johan Bedel for the help with histopathology. We
Tarantola, and Andrew Holtz for critical reading
sis illustration was created with BioRender.com.

Author contributions
JPC and HB conceived the experimental hypothes
designed the experiments. GDM, FLaz, FLar, LF, LK
the experiments. GDM, FLaz, FLar, LF, EK, SL, AM,
the data. GDM, J-PC, and HB wrote the manuscrip

Conflict of interests

metaflammation: therapeutic targets for obesity and type 2 diabetes. *Pharmacol Res* 152: 104602

Arévalo AP, Pagotto R, Pórfido Jl, Daghero H, Segovia M, Yamasaki K, Varela B, Hill M, Verdes JM, Duhalde Vega M *et al* (2021) Ivermectin reduces *in vivo* coronavirus infection in a mouse experimental model. *Sci Rep* 11: 7132

AVMA (2020) *AVMA guidelines for the euthanasia of animals: 2020 edition**. Schaumburg, IL: American Veterinary Medical Association

Baer A, Kehn-Hall K (2014) Viral concentration determination through plaque assays: using traditional and novel overlay systems. *J Vis Exp* e52065

Bastard P, Rosen LB, Zhang Q, Michailidis E, Hoffmann HH, Zhang Y, Dorgham K, Philippot Q, Rosain J, Béziat V *et al* (2020) Autoantibodies against type I IFNs in patients with life-threatening COVID-19. *Science* 370: eabd4585

Batalha PN, Forezi LSM, Lima CGS, Pauli FP, Boechat FCS, de Souza MCBV, Cunha AC, Ferreira VF, da Silva FdC (2021) Drug repurposing for the treatment of COVID-19: Pharmacological aspects and synthetic approaches. *Bioorg Chem* 106: 104488

Beco L, Petite A, Olivry T (2001) Comparison of subcutaneous ivermectin and oral moxidectin for the treatment of notoedric acariasis in hamsters. *Veterinary Record* 149: 324–327

Bernigaud C, Guillemot D, Ahmed-Belkacem A, Grimaldi-Bensouda L, Lespine A, Berry F, Softic L, Chenost C, Do-Pham G, Giraudeau B *et al* (2021) Oral ivermectin for a scabies outbreak in a long-term–care facility: potential value in preventing COVID-19 and associated mortality? *Br J Dermatol* 184: 1207–1209

Bhaskar S, Sinha A, Banach M, Mittoo S, Weissert R, Kass JS, Rajagopal S, Pai AR, Kutty S (2020) Cytokine storm in COVID-19—immunopathological mechanisms. Clinical considerations, and therapeutic approaches: the REPROGRAM consortium position paper. *Front Immunol* 11: 1648

Boudewijns R, Thibaut HJ, Kaptein SJF, Li R, Vergote V, Seldeslachts L, Van Weyenbergh J, De Keyzer C, Bervoets L, Sharma S *et al* (2020) STAT2 signaling restricts viral dissemination but drives severe pneumonia in SARS-CoV-2 infected hamsters. *Nat Commun* 11: 5838

Bray M, Rayner C, Noël F, Jans D, Wagstaff K (2020) Ivermectin and COVID-19: a report in antiviral research, widespread interest, an FDA warning, two letters to the editor and the authors' responses. *Antiviral Res* 178: 104805

Calabrese EJ, Kozumbo WJ, Kapoor R, Dhawan G, Jimenez PCL, Giordano J (2021) NRF2 activation putatively mediates clinical benefits of low-dose radiotherapy in COVID-19 pneumonia and acute respiratory distress syndrome (ards): novel mechanistic considerations. *Radiother Oncol* 160: 125–131

Caly L, Druce JD, Catton MG, Jans DA, Wagstaff KM (2020) The FDA-approved drug ivermectin inhibits the replication of SARS-CoV-2 *in vitro*. *Antiviral Res* 178: 104787

Chaccour C, Casellas A, Blanco-Di Matteo A, Pine Ruiz-Castillo P, Richardson M-A, Rodríguez-M Brew J *et al* (2021) The effect of early treatm load, symptoms and humoral response in pat COVID-19: a pilot, double-blind, placebo-cont trial. *EClinicalMedicine* 32: 100720

Chan JF, Zhang AJ, Yuan S, Poon VK, Chan CC, Le HW, Wen L *et al* (2020) Simulation of the clir manifestations of Coronavirus Disease 2019 (hamster model: implications for disease path *Clin Infect Dis* 9: 2428–2446

Changeux J-P, Amoura Z, Rey FA, Miyara M (202 Covid-19 with preventive and therapeutic im

Chen EY, Tan CM, Kou Y, Duan Q, Wang Z, Meire (2013) Enrichr: interactive and collaborative H analysis tool. *BMC Bioinformatics* 14: 128

Chen W, Pan JY (2021) Anatomical and patholog of SARS and COVID-19: microthrombosis is th *Proced Online* 23: 4

Cokelaer T, Pultz D, Harder LM, Serra-Musach J, BioServices: a common Python package to ac programmatically. *Bioinformatics* 29: 3241–32

Cokelaer T, Desvillechabrol D, Legendre R, Cardor snakemake NGS pipelines. *J Open Source Softu*

Cross SJ, Linker KE, Leslie FM (2017) Sex-depende developing brain. *J Neurosci Res* 95: 422–436

De Virgiliis F, Di Giovanni S (2020) Lung innervat storm: neuroimmune interactions and COVID 645–652

Dey A, Sen S, Maulik U (2020) Unveiling COVID-1 cell types and cell-specific pathway cascade.

Dobin A, Davis CA, Schlesinger F, Drenkow J, Zale Chaisson M, Gingeras TR (2012) STAR: ultrafa *Bioinformatics* 29: 15–21

Ewels P, Magnusson M, Lundin S, Käller M (2016 analysis results for multiple tools and sample *Bioinformatics* 32: 3047–3048

Gahring LC, Myers EJ, Dunn DM, Weiss RB, Roge 7 receptor expression and modulation of the lipopolysaccharide. *PLoS One* 12: e0175367

Galani IE, Triantafyllia V, Eleminiadou E-E, Koltsi Manioudaki M, Thanos D, Doyle SE, Kotenko S (2017) Interferon-λ mediates non-redundant against influenza virus infection without com *Immunity* 46: 875–890.e6

Hasanoglu I, Korukluoglu G, Asilturk D, Cosgun Y, Kalem AK, Altas AB, Kayaaslan B, Eser F, Kuzucu EA, Guner R (2021) Higher viral loads in asymptomatic COVID-19 patients might be the invisible part of the iceberg. *Infection* 49: 117–126

Heidary F, Gharebaghi R (2020) Ivermectin: a systematic review from antiviral effects to COVID-19 complementary regimen. *J Antibiot* 73: 593–602

Hibbs RE, Gouaux E (2011) Principles of activation and permeation in an anion-selective Cys-loop receptor. *Nature* 474: 54–60

Hill A, Abdulamir A, Ahmed S, Asghar A, Babalola OE, Basri R, Chaccour C, Chachar AZK, Chowdhury ATM, Elgazzar A *et al* (2021) Meta-analysis of randomized trials of ivermectin to treat SARS-CoV-2 infection. *Res Squ* https://doi.org/10.21203/rs.3.rs-148845/v1 [PREPRINT]

Hoagland DA, Møller R, Uhl SA, Oishi K, Frere J, Golynker I, Horiuchi S, Panis M, Blanco-Melo D, Sachs D *et al* (2020) Leveraging the antiviral type-I interferon system as a first line defense against SARS-CoV-2 pathogenicity. *Immunity* 54: 557–570

Horby P, Lim WS, Emberson JR, Mafham M, Bell JL, Linsell L, Staplin N, Brightling C, Ustianowski A, Elmahi E *et al* (2020) Dexamethasone in hospitalized patients with Covid-19 - preliminary report. *N Engl J Med* 384: 693–704

Hu X, Cai X, Song X, Li C, Zhao J, Luo W, Zhang Q, Ekumi IO, He Z (2020) Possible SARS-coronavirus 2 inhibitor revealed by simulated molecular docking to viral main protease and host toll-like receptor. *Future Virol* 15: 359–368

Huntley RP, Sawford T, Mutowo-Meullenet P, Shypitsyna A, Bonilla C, Martin MJ, O'Donovan C (2014) The GOA database: gene ontology annotation updates for 2015. *Nucleic Acids Res* 43: D1057–D1063

Isidori AM, Giannetta E, Pofi R, Venneri MA, Gianfrilli D, Campolo F, Mastroianni CM, Lenzi A, d'Ettorre G (2021) Targeting the NO-cGMP-PDE5 pathway in COVID-19 infection. The DEDALO project. *Andrology* 9: 33–38

Islam T, Rahman MR, Aydin B, Beklen H, Arga KY, Shahjaman M (2020) Integrative transcriptomics analysis of lung epithelial cells and identification of repurposable drug candidates for COVID-19. *Eur J Pharmacol* 887: 173594

Jermain B, Hanafin PO, Cao Y, Lifschitz A, Lanusse C, Rao GG (2020) Development of a minimal physiologically-based pharmacokinetic model to simulate lung exposure in humans following oral administration of ivermectin for COVID-19 drug repurposing. *J Pharm Sci* 109: 3574–3578

Jin J-M, Bai P, He W, Wu F, Liu X-F, Han D-M, Liu S, Yang J-K (2020) Gender differences in patients with COVID-19: focus on severity and mortality. *Frontiers in Public Health* 8: 152

Kanehisa M, Goto S (2000) KEGG: kyoto encyclopedia of genes and genomes. *Nucleic Acids Res* 28: 27–30

Kaur H, Shekhar N, Sharma S, Sarma P, Prakash A, Medhi B (2021) Ivermectin as a potential drug for treatment of COVID-19: an in-sync review with

Laing R, Gillan V, Devaney E (2017) Ivermectin – *Parasitol* 33: 463–472

Lazarini F, Gabellec M-M, Torquet N, Lledo P-M microglia triggers long-lasting impairment of olfactory bulb. *The Journal of Neuroscience* 32:

Li N, Zhao L, Zhan X (2021) Quantitative proteor spectrum antiviral property of ivermectin, be treatment. *J Cell Physiol* 236: 2959–2975

Liao Y, Smyth GK, Shi W (2014) featureCounts: a program for assigning sequence reads to gen 30: 923–930

Lifschitz A, Virkel G, Sallovitz J, Sutra JF, Galtier F (2000) Comparative distribution of ivermectir location tissues in cattle. *Vet Parasitol* 87: 327

Love MI, Huber W, Anders S (2014) Moderated e dispersion for RNA-seq data with DESeq2. *Ge*

Martin M (2011) Cutadapt removes adapter sequ sequencing reads. *EMBnet J* 17: 10

Masood KI, Mahmood SF, Shahid S, Nasir N, Gha Khanum I, Razzak S, Kanji A *et al* (2020) Tran disease severity in patients with COVID-19 re and vasculature related genes. *medRxiv* https 20132571 [PREPRINT]

McElvaney OJ, Hobbs BD, Qiao D, McElvaney OF, O'Connor E, Walsh S, Cho MH *et al* (2020a) A based on the ratio of interleukin-6 to interleu COVID-19. *EBioMedicine* 61: 103026

McElvaney OJ, McEvoy NL, McElvaney OF, Carrol DM, Ní Choileáin O, Clarke J, O'Connor E, Hog Characterization of the inflammatory respons *Am J Respir Crit Care Med* 202: 812–821

de Melo GD, Lazarini F, Levallois S, Hautefort C Verillaud B, Aparicio C, Wagner S, Gheusi G related anosmia is associated with viral per in human olfactory epithelium and brain in *Transl Med* 13: eabf8396

Melotti A, Mas C, Kuciak M, Lorente-Trigos A, Bo The river blindness drug Ivermectin and relat inhibit WNT-TCF pathway responses in huma 1263–1278

Mi H, Muruganujan A, Ebert D, Huang X, Thoma 14: more genomes, a new PANTHER GO-slim enrichment analysis tools. *Nucleic Acids Res* 4

Muñoz-Fontela C, Dowling WE, Funnell SGP, Gse Albrecht RA, Andersen H, Baric RS, Carroll MV

Pei J, Xiao Z, Guo Z, Pei Y, Wei S, Wu H, Wang D (2020) Sustained stimulation of β(2)AR inhibits insulin signaling in H9C2 cardiomyoblast cells through the PKA-dependent signaling pathway. *Diabetes Metab Syndr Obes* 13: 3887–3898

Pfaffl MW (2001) A new mathematical model for relative quantification in real-time RT-PCR. *Nucleic Acids Res* 29: e45

Potus F, Mai V, Lebret M, Malenfant S, Breton-Gagnon E, Lajoie AC, Boucherat O, Bonnet S, Provencher S (2020) Novel insights on the pulmonary vascular consequences of COVID-19. *Am J Physiol Lung Cell Mol Physiol* 319: L277–L288

Qiu C, Cui C, Hautefort C, Haehner A, Zhao J, Yao Qi, Zeng H, Nisenbaum EJ, Liu Li, Zhao Yu *et al* (2020) Olfactory and gustatory dysfunction as an early identifier of COVID-19 in adults and children: an international multicenter study. *Otolaryngol Head Neck Surg* 163: 714–721

Rajter JC, Sherman MS, Fatteh N, Vogel F, Sacks J, Rajter J-J (2020) Use of ivermectin is associated with lower mortality in hospitalized patients with COVID-19 (ICON study). *Chest* 159: 85–92

Raker VK, Becker C, Steinbrink K (2016) The cAMP pathway as therapeutic target in autoimmune and inflammatory diseases. *Front Immunol* 7: 123

Raslan AA, Yoon JK (2020) WNT signaling in lung repair and regeneration. *Mol Cells* 43: 774–783

Rossotti R, Travi G, Ughi N, Corradin M, Baiguera C, Fumagalli R, Bottiroli M, Mondino M, Merli M, Bellone A *et al* (2020) Safety and efficacy of anti-il6-receptor tocilizumab use in severe and critical patients affected by coronavirus disease 2019: A comparative analysis. *J Infect* 81: e11–e17

Said SI (1999) Glutamate receptors and asthmatic airway disease. *Trends Pharmacol Sci* 20: 132–135

Sajid MS, Iqbal Z, Muhammad G, Iqbal MU (2006) Immunomodulatory effect of various anti-parasitics: a review. *Parasitology* 132: 301–313

Samuel RM, Majd H, Richter MN, Ghazizadeh Z, Zekavat SM, Navickas A, Ramirez JT, Asgharian H, Simoneau CR, Bonser LR *et al* (2020) Androgen signaling regulates SARS-CoV-2 receptor levels and is associated with severe COVID-19 symptoms in men. *Cell Stem Cell* 27: 876–889.e12

Sang Y, Miller LC, Blecha F (2015) Macrophage polarization in virus-host interactions. *J Clin Cell Immunol* 6: 311

Scully EP, Haverfield J, Ursin RL, Tannenbaum C, Klein SL (2020) Considering how biological sex impacts immune responses and COVID-19 outcomes. *Nat Rev Immunol* 20: 442–447

Sia SF, Yan L-M, Chin AWH, Fung K, Choy K-T, Wong AYL, Kaewpreedee P, Perera RAPM, Poon LLM, Nicholls JM *et al* (2020) Pathogenesis and transmission of SARS-CoV-2 in golden hamsters. *Nature* 583: 834–838

Stanifer ML, Guo C, Doldan P, Boulant S (2020) Importance of type I and III interferons at respiratory and intestinal barrier surfaces. *Front Immunol* 11: 608645

vom Steeg LG, Klein SL (2019) Sex and sex steroids impact influenza

Suo T, Liu X, Feng J, Guo M, Hu W, Guo D, Ullah *et al* (2020) ddPCR: a more accurate tool for viral load specimens. *Emerg Microbes Infect* 9

Takahashi T, Ellingson MK, Wong P, Israelow B Mao T, Oh JE, Tokuyama M *et al* (2020) Se responses that underlie COVID-19 disease o 315–320

Tizabi Y, Getachew B, Copeland RL, Aschner M (2 nicotinic cholinergic system in COVID-19. *FEB*

Vaduganathan M, Vardeny O, Michel T, McMurra SD (2020) Renin–angiotensin–aldosterone sys with covid-19. *N Engl J Med* 382: 1653–1659

Van Den Eynden J, SahebAli S, Horwood N, Carm Steels P, Harvey R, Rigo J-M (2009) Glycine ar in non-neuronal cells. *Front Mol Neurosci* 2: 9

Varet H, Brillet-Guéguen L, Coppée JY, Dillies MA and EdgeR-based R pipeline for comprehensi RNA-Seq data. *PLoS One* 11: e0157022

WHO (2020) *Protocol: real-time RT-PCR assays fo* Paris: Institut Pasteur. https://www.who.int/d viruse/real-time-rt-pcr-assays-for-the-detectic steur-paris.pdf?sfvrsn=3662fcb6_2

Xydakis MS, Dehgani-Mobaraki P, Holbrook EH, Hautefort C, Herman P, Manley GT, Lyon DM, taste dysfunction in patients with COVID-19. 1016

Zemkova H, Tvrdonova V, Bhattacharya A, Jindric modulation of ligand gated ion channels by i (Suppl 1): S215–S224

Zhang Q, Bastard P, Liu Z, Le Pen J, Moncada-Sabli IKD, Hodeib S, Korol C *et al* (2020a) In immunity in patients with life-threatening eabd4570

Zhang SI, Liu Y, Wang X, Yang LI, Li H, Wang Y, I *et al* (2020b) SARS-CoV-2 binds platelet ACE2 COVID-19. *J Hematol Oncol* 13: 120

Zhao X, Yu Z, Lv Z, Meng L, Xu J, Yuan S, Fu Z (2 nicotinic acetylcholine receptors (α7nAchR) p autophagy in LPS-induced acute lung injury *Inflammation* 42: 2236–2245

Zhe Z, Hongyuan B, Wenjuan Q, Peng W, Xiaowe glutamate receptor ameliorates lipopolysacch regulation of neuropeptides. *Biosci Rep* 38: BS